

3. Tribology Fundamentals

Our research on confined materials has been strongly influenced by our work in nanotribology. Tribology, although one of the oldest engineering discipline, it is one of the least developed classical sciences to date. The reason is that Tribology like Nanoscience is neither truly a single discipline nor well represented by steady state processes. It involves all the complexities of nano-constrained materials that are experienced over a wide range of scales during a shear occurrence.

Originally, idealized solid lubricant films, such as Langmuir Blodgett (LB) films, served as model systems. Thus, first insight into nanoscopic friction processes were revealed on phase separated monolayer systems, as illustrated in Fig. 3-1.⁵ For that reason, we pioneered a SPM based tool that is known today as friction force microscopy (FFM). Our early studies involved various aspects in friction, lubrication, wear and adhesion.^{5,9,19-25} The two most influential were the nanoscopic distinction and visualization of material phases,⁵ and the first measurement of a truly molecular stick-slip process that was thought, at that time, to manifest the origin of “wearless” friction,²³ Fig. 3-2. The nanoscopic distinction of material phases led later to an entire subdiscipline in nanoscience probing, referred to as “chemical force microscopy”. The wearless molecular scale friction study that confirmed the old Prandtl-Tomlinson molecular stick-slip model from the 1930s, led to various theoretical developments that currently form the state-of-the-art understanding of molecular scale friction, an aspect that is critically assessed and redirected towards intrinsic material properties in our current research (see following subsection).

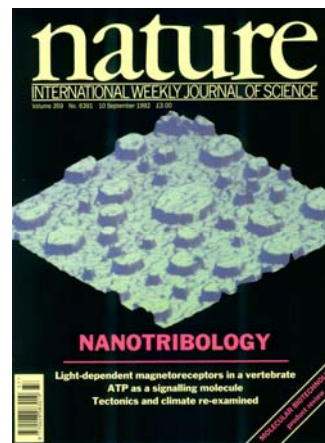


Fig. 3-1: Friction on phase separated monolayer.⁵

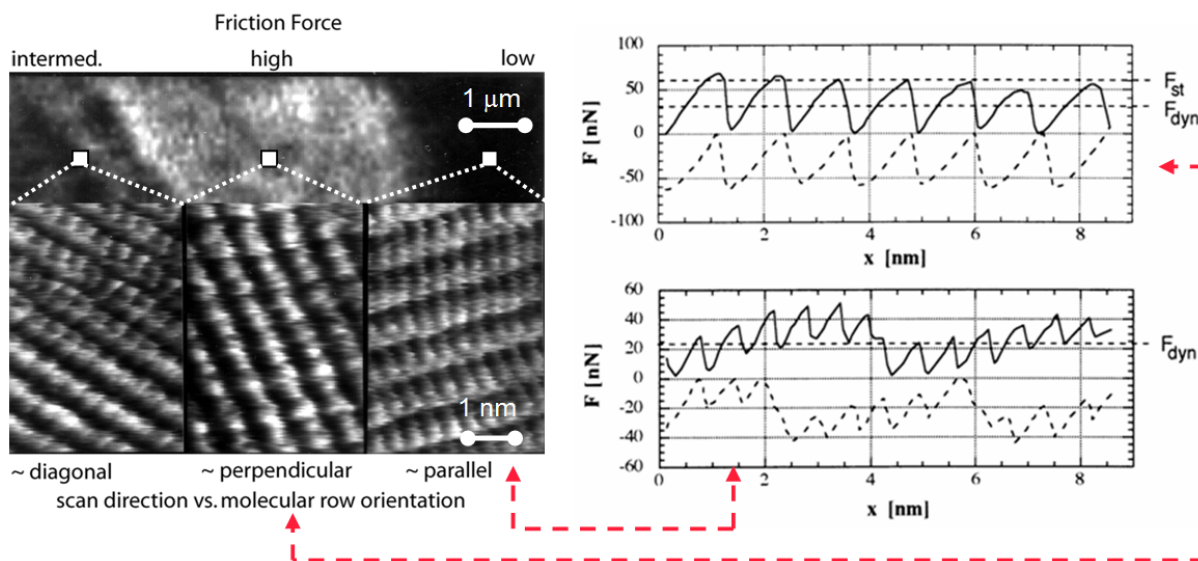


Fig. 3-2: FFM molecular stick-slip study of a bilayer lipid system (5-(4'-N,N-dihexadecylamino)benzylidene barbituric acid). (Left) Macroscopic friction force contrasts (top) are related to the relative alignment of the molecular structure (bottom) in respect to the left-to-right scanning direction. The orientation of the anisotropic row-like structure dictates the friction force values (contrast). (Right) Friction hysteresis curves for “perpendicular (top) and more or less “parallel” sliding directions (bottom). F_{st} , static friction, is assigned to the maximum force occurrence. The average stick-slip value F_{dyn} corresponds to the dynamic friction value determined on large scale micrometer scans.²³

With our increasing involvement in polymers and fluids, our attention in tribology related aspects turned to confinement effect in thin solid polymer films^{1,3,4,7,8,10,12,16,18,26-32} and interfacially

confined liquids^{2,13,33,34}. In particular one aspect defined our group's research in tribology over the recent years. It is the true material origin for friction dissipation in condensed matter.

In general, tribology research, and I include here most of the experimental and theoretical research that has been conducted, has merely focused on a descriptive formalism of the tribological process. This claim can easily be justified if one tries to cognitively synthesize a lubricant molecule based on fundamental research results. It is unattainable, as the information available concerning the friction dissipation process is not linked to the molecules themselves, but only to generic models or processes. With the discussion above (Figure 3-2), I provided an example of a generic dissipation process – the stick-slip behavior – as illustrated in Fig. 3-3 in its simplest form. Note, there is no information provided in how the material itself is actually involved in dissipating the energy.

Current molecular models in tribology that go beyond the simplistic Prandtl-Tomlinson Model (Fig. 3-3) are still only employing Langevin equations and Fokker-Planck statistical kernels, and thus, focus on generic periodic potentials that are thermally and mechanically inert. Energy dissipation is described primarily only by viscous dampeners and heat generation, without gaining insight into the molecular dissipation process involving material intrinsic molecular or submolecular modes of relaxation. Thus, effective molecular models necessary to design the next generation of low dissipation tribological interfaces from the bottom-up are missing.

The opportunity to observe and consequently engineer the energy transfer from the one-dimensional frictional sliding motion into the multi-dimensional phase state close to the material's equilibrium condition embodies the main motivation of our current research effort. With the experience and insight our group has gained over the years in nanorheology of confined organic material systems, we started to pursue a path that treats tribological systems in terms of activated processes, involving reaction kinetics and rheology, with activation barriers that are specific to the material involved. This concept and our involvements are described for organic solids and liquids in the following sections.

3.1 Tribo-Dissipation Involving Intramolecular Constraints

An effective material design concept in tribology involves material synthesis that is tailored from the bottom-up (submolecular scale) towards the desired properties and functionalities. This involves insight into the material behavior under shear stress sliding conditions.

Since Bowden and Tabor's adhesive-concept of energy dissipation, friction has been dealt with from a surface science perspective involving a variety of process descriptions (e.g., wear phenomena and stick-slip processes, and tribochemistry), while material specific relaxation properties moved more into the background. Interestingly, it was Tabor who was one of the pioneers besides Grosch, in considering molecular relaxation properties responsible for energy dissipation in polymer rubbers.³⁵ This *triborheological description* of frictional dissipation faced significant resistance by *surface bonding-debonding theories* pioneered by Schallamach and others.³⁵ One of the shortcomings of triborheological description in 1950-60 was the inability to specifically excite material intrinsic molecular modes of relaxations during phenomenological sliding motions. Large and rough contact regimes imposed convoluted signals containing aspects of sliding and cutting among others, and trapped the slow relaxing polymer phases in non-equilibrium states. Also, the material within the interfacial sliding region was rather poorly defined.

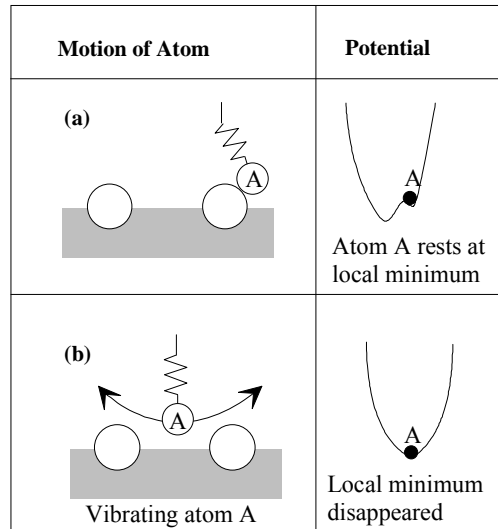


Fig. 3-3: Generic Friction Model by Prandtl and Tomlinson

In contrast to the macro-techniques used by Tabor and others, the ability to probe a material closer to its equilibrium has been a hallmark of scanning force microscopy (SFM), as already addressed above. In one of our more recent SFM friction studies on atactic and monodisperse polystyrene (PS),²⁸ involving IFA,^{*} we showed that the sliding motion can couple to very specific submolecular rotational motions within the material, as illustrated in Fig. 3-4 for the phenyl rotation at the PS backbone.

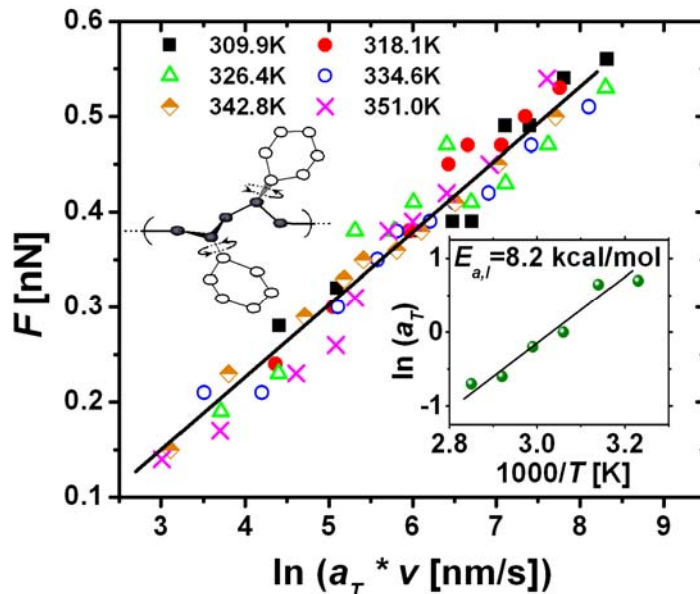


Fig. 3-4: Intrinsic friction analysis (IFA) of polystyrene below the glass transition and at low probing pressure ($L < L^*$) reveals an activation barrier $E_{a,l}$ of 8.2 kcal/mol (phenyl rotation).^{1,28}

The coupling of the sliding motion with actuators of the material's relaxation states gave rise to a barrier-hopping fluctuation not unlike the one observed for highly ordered surfaces. Friction-rate isotherms obtained with a SFM tip on glassy polystyrene could also be collapsed to a master curve according to a tribological *ramped* creep model by Dudko and Sang,²⁸ which considers a single asperity sliding over a corrugated surface potential that is biased due to the motion of the driven tip.

Ramped creep scaling is consistent with the solution of the Langevin equation for a perfect cantilever oscillator, i.e.,

$$M\ddot{x} + M\beta\dot{x} + \frac{\partial E(x,t)}{\partial x} = \xi(t), \quad (3.1)$$

with the total potential energy E , the position of the tip on the surface x , the mass of tip M , the linear dampening factor β , and the thermal noise in the form of the random force $\xi(t)$, where $\langle \xi(t)\xi(t') \rangle \propto k_B T \delta(t-t')$. Eq. 3.1 is based on a sinusoidal surface potential continuously overcome during the course of frictional sliding. The challenge is the experimental determination of the energy barrier E , which provides intrinsic information about the material involved. For example, we determined by IFA an energy potential under low pressure conditions of 8.2 ± 1 kcal/mol for glassy polystyrene that could be assigned to the hindered rotation of the phenyl ring side chains about their bond with the backbone.^{1,28} In this study, friction could be directly linked to the "molecular deformation properties" (side-chain relaxations) of the underlying molecular building blocks.

Thus, nanoscale friction-rate isotherms, if treated according to the WLF superposition principle (c.f. sec. 1.2), provide submolecular scale information about the relaxation modes available. This information can be (i) used to access the dissipative process on a submolecular

* For details about IFA see section 1.

scale, and/or (ii) fed back into the manufacturing design process to either cognitively affect the molecular synthesis or material processing.

To put the PS study above (Fig. 3-4) in perspective to a classical tribological analysis, I present with Figure 3-5 phenomenological friction-load curves, $F(L)$, over a range of temperatures ($T < T_g$) and scan velocities. The first thing, we notice, is the wealth of information in this plot. Below T_g , each of the $F(L)$ isotherms reveals a kink at a critical normal load, $L^*(T)$, separating each curve into two linear friction-load branches with friction coefficients $\mu_I(T)$ and $\mu_{II}(T)$. This phenomenon is apparent with variations in both temperature and scan rate (Fig. 3-5 inset). It is important to note that the absolute values of L^* are dependent on the applied pressure, i.e., involve besides the applied load also the cantilever tip size. The friction force at the critical load, $F^*(L^*(T,v))$, reveals a linear and logarithmic dependence with temperature and velocity, respectively, as expected from thermodynamic friction models

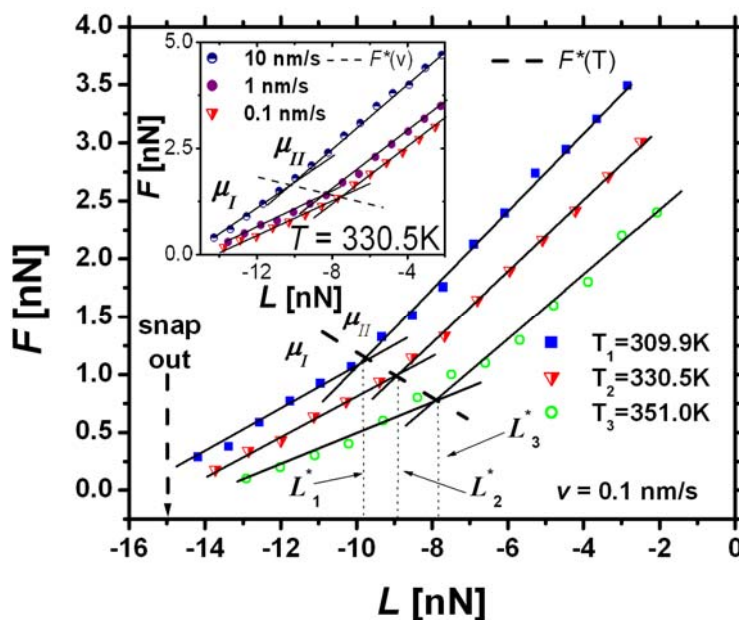


Fig. 3-5: Isothermal friction-load plots for atactic PS subdivided at critical loads L_k^* ($k = 1, 2, 3$) into two friction regimes with friction coefficients μ_I and μ_{II} . The dashed line tracks critical loads; i.e., $F^*(T) = F_{o,T} - \alpha T$, with $\alpha = 8.5$ pN/K and $F_{o,T} = 3.7$ nN. (Inset) Friction-load plots at constant temperature with $F^*(v) = F_{o,v} + \beta \ln v$ (dashed line), where $\beta = 0.076$ nN and $F_{o,v} = 1.5$ nN.¹

To elucidate the molecular origin for the two friction regimes, we individually employed IFA to the μ -specific branches of the isotherms. The study revealed two apparent activation energies $E_{a,I} = 8.2 \pm 1$ kcal/mol (~ 0.30 eV) and $E_{a,II} = 21.7 \pm 2$ kcal/mol (~ 0.94 eV) below and above the critical load $L^*(T)$, respectively, as shown in Fig. 3-4 and Fig. 3-6. Hence, the cause for the discontinuity in the friction-load curve in Figure 3-5 was found to originate from a transition between two loading (more precisely – pressure) dependent material specific relaxation modes.¹ The known preferential orientation of the phenyl pendant groups towards the free-surface normal explains why these two modes are separated by a well-defined transition load. As illustrated in Figure 3-7, at low load, the phenyls act like surface ball bearings lowering the frictional dissipation significantly. At specific, temperature and velocity dependent critical loads, the phenyls are displaced and the ‘subsurface’ or bulk relaxation mode, i.e., the translational crankshaft motion, takes over as the primary dissipation mechanism. This leads to a significant increase in energy dissipation that is caused to a large extent by molecular cooperativity. The transition forces $F^*(v)$ and $F^*(T)$ (see Fig. 3-5) can also be analyzed in a manner analogous to the IFA energy analysis presented above in accordance with the superposition principle. We deduced from $F^*(v)|_{T=}$

isotherms an activation energy of 9.9 ± 1 kcal/mol, which reflects the phenyl loading capacity at the free surface.

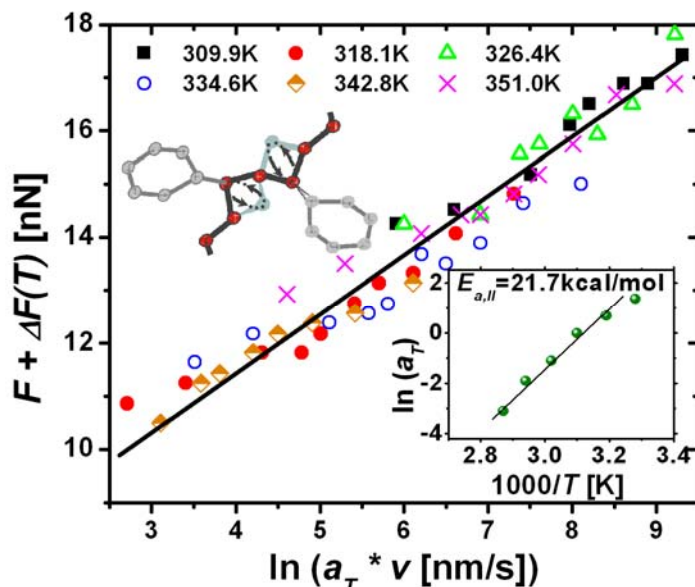


Fig. 3-6: Intrinsic friction analysis (IFA) of polystyrene below the glass transition and at high probing pressure ($L > L^*$) reveals an activation barrier $E_{a,I}$ of 21.7 kcal/mol (isolated polymer backbone motion).¹

As pointed already out in section 1, the apparent activation barrier contains an enthalpic and entropic component. While the enthalpic component provides the activation barrier for submolecular rotations and segmental translations, the entropic component provides a measure of the cooperative motion involved, also illustrated in Fig. 1-5. The entropic component $T_R \Delta S$ can be a significant contributor to the total frictional energy dissipation.[†] In the case of the translational crankshaft motion of PS, it raises the energy that is dissipated by 20%.¹ Above the glass transition this number even quadruples.¹ It is important to note that such contributions are omitted by enthalpic friction models based on Eq. 3-1 with $\langle \xi(t) \xi(t') \rangle \propto k_B T \delta(t-t')$ that consider only uncoordinated energy dissipation processes. Based on Eq. 1.6 and a thermal activation model discussed in more detail in the next subsection, we derived an analytical relationship between the experimental IFA observable for cooperativity ΔF (vertical shift - see section 1, Figs 1-2 and 1-6) and $T_R \Delta S$, which can be approximated by its significant components, as¹

$$\Delta F \approx -\frac{T_R \Delta S}{\phi} A. \quad (3.2)$$

Here, A represents the area of contact and ϕ the stress activation volume, a measure of the spatial effect of cooperativity.

This study illustrates our efforts in attaining a truly fundamental understanding of friction dissipation processes of mechanically compliant material. Further progress in this area will provide us with the means to design molecules (possibly assisted by computer simulation) with submolecular scale prescribed frictional energy dissipation characteristics.

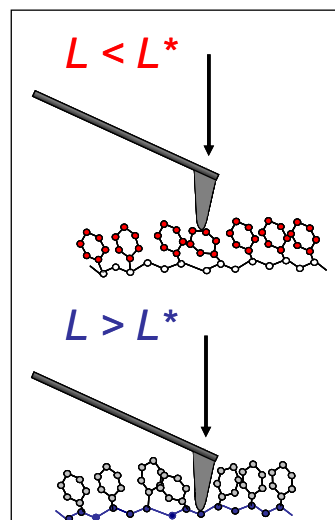


Fig. 3-7: Phenyl dominated surface. L^* resembles a sub-molecular critical load "capacity".

[†] See subsection 1.2 (Fig. 1-5) for the definition of the reduced temperature T_R .

3.2 Liquid-Lubrication: Molecular, Interfacial and Dimensional Constraints

Contrary to dry or solid-lubrication, there has been since Reynolds in the late nineteenth century, a much better understanding developed regarding energy dissipation during sliding in liquids than in solids. The reason for the early success in obtaining improved basic insight into liquid lubrication is due to the incorporation of underlying fundamental theories such as fluid mechanics, rheology, and thermodynamics. This has been in general, as pointed out above, the shortcoming of dry friction analysis.

It is well known that the frictional resistance between solids is significantly reduced if lubricated. Various characteristic velocity dependencies have been found for liquid lubrication depending on the lubricant thickness (or more generally on the Gumbel number). In surface forces apparatus (SFA) and in our SFM studies,¹³ it has been shown that friction involving liquids can exhibit a logarithmic behavior in velocity, which is contrary to Reynolds linear creep relationship. This transient behavior of liquids finds its counterpart in dry or solid-lubrication, where logarithmic behaviors have also been reported, as discussed above.

From a thermodynamic point of view, sliding discontinuities are caused by activation barriers, which are repeatedly overcome during the sliding process. Utilizing a thermodynamic activation model that goes back to Eyring (refined by Briscoe ~1980), we analyzed the energy dissipation process involving the "simple" liquids, n-hexadecane ($n\text{-C}_{16}\text{H}_{34}$) and octamethylcyclotetrasiloxane (OMCTS).² As opposing solid surfaces served silicon-oxide nanoscale sharp SFM tips and ultrasmooth planar silicon-oxide wafers (5 Å roughness). The two liquids have been selected based on their similar chemical affinity to silicon, with distinctly different molecular shape; i.e., linear chain ($n\text{-C}_{16}\text{H}_{34}$) vs. spherically shaped (OMCTS) molecules. We examined the degree of interfacial liquid structuring (c.f. sec. 2.3), and its contribution to localized shear processes. While shear approach curves provided the thickness of entropically cooled boundary layers, Fig. 2-7, a thermomechanical analysis involving friction-velocity data, as presented in Figure 3-8, reveals distinctly different tribological responses.

Friction-velocity plots were obtained with SFM cantilevers that were fully immersed in the liquid lubricant and scanned with a one $\mu\text{m/s}$ -velocity in an apparent contact with a silicon surface at constant load and temperature.² As documented in Figure 3-8, logarithmic friction-velocity relationships, $F_F(v) = F_o + \alpha \ln(v[\mu\text{m/s}])$, were found for n-hexadecane and OMCTS. The measurements are compared to "dry" $\text{SiO}_x\text{-SiO}_x$ contact sliding at 18 % relative humidity. Surprisingly on first sight, n-hexadecane exceeds OMCTS in its performance as a lubricant for asperity sliding within the observed velocity and temperature ranges. This result was unexpected at first as the OMCTS bulk viscosity is 30 % lower in comparison to n-hexadecane. After a modulated shear analysis (c.f. sec. 2.3), it became

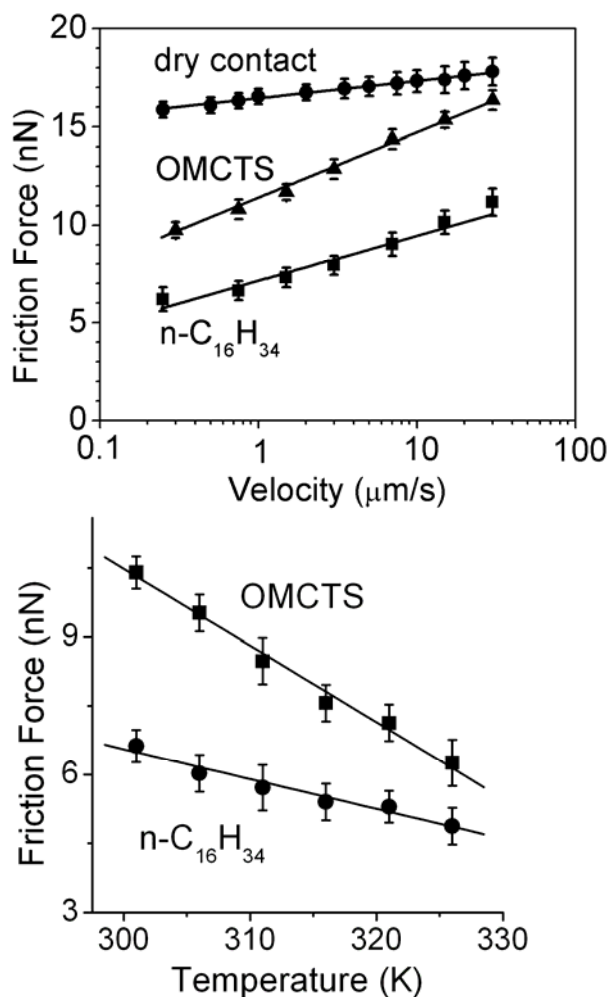


Fig. 3-8: FFM measurements of n-hexadecane and OMCTS as function of velocity (top) and temperature (bottom).²

clear that the bulk-modified boundary layer of n-hexadecane was responsible for improved lubrication properties.

To analyze the lubrication process from an energetic perspective, we expressed the shear velocity as

$$v = v_o e^{-E_a'/(k_B T_R)}, \quad (3.3)$$

with the relaxation temperature T_R , and the apparent Arrhenius activation energy of the form

$$E_a' = Q' + P\Omega - \tau\phi. \quad (3.4)$$

As illustrated in Figure 3-9, Q' is the potential barrier height with respect to the plastic deformation, P is the pressure imposed, Ω is the pressure activation volume, τ is the shear stress, and ϕ is the stress activation volume. With this *Ansatz*,

we followed Eyring's footsteps and discussed the liquid at rest in terms of a thermal activation model, wherein the individual liquid molecules experience a "cage-like" barrier that hinders molecular free motion, because of the close packing in liquids. The stress activation volume ϕ can be conceived as a process coherence volume, and interpreted as the size of the moving segment in the unit shear process, whether it is a part of a molecule or a dislocation line. This model yields for the stress,²

$$\tau = \tau_o' - \beta T, \quad (3.5)$$

a linear relationship with temperature, and

$$\tau = \frac{k_B T}{\phi} \ln\left(\frac{v}{v_o}\right) + \frac{1}{\phi}(Q + P\Omega), \quad (3.6)$$

a logarithmic relationship with the scan velocity. Both are in accordance with our experiments, Fig. 3-8. Considering that the shear strength can be expressed as the friction force, $F_F(v) = F_o + \alpha \ln(v[\mu\text{m/s}])$, per unit area A , the following equation can be directly derived from Eq. (3.6) for constant temperature and pressure:

$$\frac{\phi}{A} = \frac{k_B T}{\alpha}. \quad (3.7)$$

The normalized stress activation volume of our study is provided in Fig. 3-10. As expected, the stress activation length (or coherence length) in a dry contact situation dominates the ones in lubricated junction. However it has to be pointed out that the origin of the activation barrier (or jump probability) in dry SFM friction experiments of incompressible material is not just caused by phonon excitations in the material, which are too fast to be observable, but by instability jumps (stick-slip) of the cantilever tip,²³ as addressed at the beginning of this section. To what extent lubricated SFM tip-sliding measurements reflect trapping probabilities is unknown. As there is a recognizable difference in the stress activation length between n-hexadecane and OMCTS (Fig. 3-10), for two liquids with similar chemical affinity and bulk rheology, we can conclude that the intrinsic molecular response time of the liquid (i.e. self-diffusion) is in part responsible for the liquid-specific $F_F(v)$ relationship. In other words, n-hexadecane shows higher stress coordination than OMCTS. This interpretation is in accordance with the modulated approach measurements presented in section 2.3.

Studies such as this illuminate constraints imposed on liquids in the interfacial regime. They provide insight into the activation energies involved. In this particular case, we estimated based

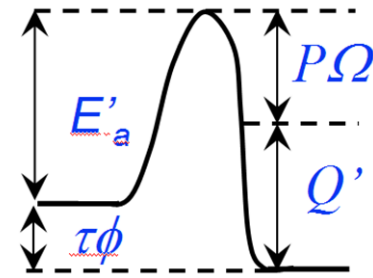


Fig. 3-9: Thermodynamic shear activation model.

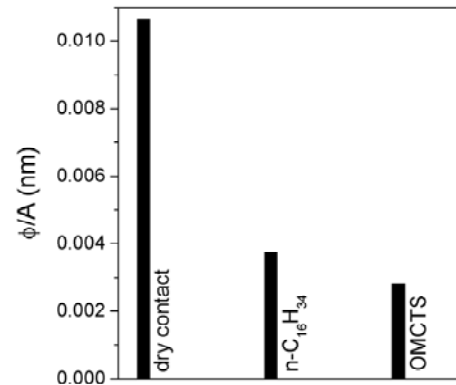


Fig. 3-10: Stress activation volume – a measure of the stress coordination.

on the characteristic velocity, $v_0=vd$ (composed of the process frequency, v , and a jump distance, d) the process activation energy Q to be on the order of 10^{-20} J.²³ Although the entropically cooled boundary layer is far from freezing, it shall be noted that the heat of fusion at the melting point is 1.99×10^{-20} J and 8.85×10^{-20} J for OMCTS and n-hexadecane, respectively. Thus, shear induced phase/structural changes are very likely to occur.

In summary, our research in liquid lubrication has focused on intrinsic constraints, and shear deformation. We have tried to avoid external pressure induced constraints (i.e., molecule trapping), and thus, have stayed as close as possible to the material equilibrated state. The research presented here gave us insight into molecular-shape-induced structuring if dimensional constraints are involved. It also showed the strong impact on frictional dissipation, which cannot be explained by viscometric data. Research that is on-going and planned will also involve to a greater degree temperature and size effects.

3.3 Two-Dimensional Polymer Liquids and Reaction Kinetics

Our research has been addressing over the years many aspects involving monolayer systems.^{5,9,13,19,20,22-25,36-40} Of recent interest has been the interplay between thermomechanical properties of monolayers and their reaction kinetics towards substrates. This has shown to be of great importance, for instance, in hard drive lubrication involving “smart” lubricant monolayers, where the molecules have to backfill very quickly any lubricant layer defects after a slider impacts.

In collaboration with IBM we have studied the molecular mobility of hydroxyl-terminated perfluoropolyether (PFPE-OH) monolayer films, Fig. 3-11 that are widely used in lubrication of magnetic storage devices. These fluids exhibit spatially terraced flow profiles indicative of film layering, and a spreading dynamics that is diffusive in nature. In magnetic storage devices the hydroxylated chain ends of molecularly-thin PFPE-OH films interact with the solid surface, an amorphous carbon surface, via the formation of hydrogen-bonds with the polar, carbon-oxygen functionalities located on the carbon surface. The bonding of the PFPE-OH polymer to carbon depends on the ability of the PFPE backbone to spatially deliver the hydroxyl end-group to within a sufficiently close distance to the surface active sites.

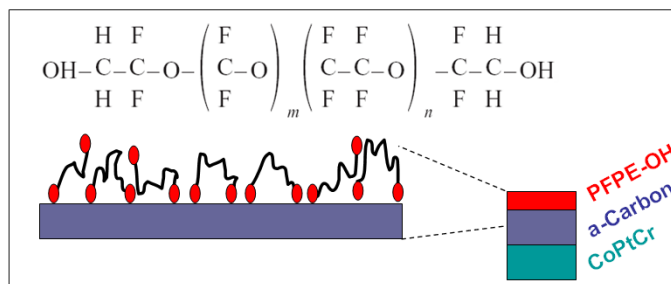


Fig. 3-11: PFPE-OH monolayer lubrication of wear protective amorphous carbon (a-Carbon) layer. Chemical formula Fomblin ZDOL[®], a widely used PFPE-OH polymer.[‡]

Kinetic measurements probing the bonding of the PFPE-OH polymer to the carbon reveal two distinctive kinetic behaviors. Below 56 °C the kinetics are described with a time-dependent rate coefficient of the form $k(t) = k_b t^{-1/2}$ and at temperatures above 85 °C with $k(t) = k_b t^{-1}$. Our kinetic experiments reveal an abrupt increase in the bonding rate constants, k_B , above ~50 °C as illustrated in Fig. 3-12.

The bonding kinetics in the low-temperature regime is characteristic of a diffusion-limited reaction occurring from a glass-like state of the molecularly-thin PFPE-OH film. The mobility of the PFPE chain in the glass-like state is limited by the propagation of holes, or packets of free volume, which facilitate configurational rearrangements of the chain. The onset of changes in the

[‡] Fomblin ZDOL[®] is a random copolymer of perfluorinated ethylene oxide and perfluorinated methylene oxide

bonding kinetics at nominally $T > 56^\circ$ signifies a fundamental change in the mobility of the molecularly thin PFPE-OH film. Specifically, the transition in the fractal time dependence suggests that delivery of the hydroxyl moiety to the surface is no longer limited by hole diffusion, and the increase in the initial rate constant indicates an enhancement in the backbone flexibility. These results are consistent with a transition in the film from a glass-like to a liquid-like state, as illustrated in Fig. 3-13, where the enhanced PFPE-OH segmental mobility results from rotations about the ether oxygen linkages in the chain that become increasingly facile. The time dependence observed in the high-temperature rate coefficients, $k(t) = k_b t^{-1}$, is characteristic of a process occurring from a confined liquid-like state in which the activation energy increases as the extent of the reaction increases.

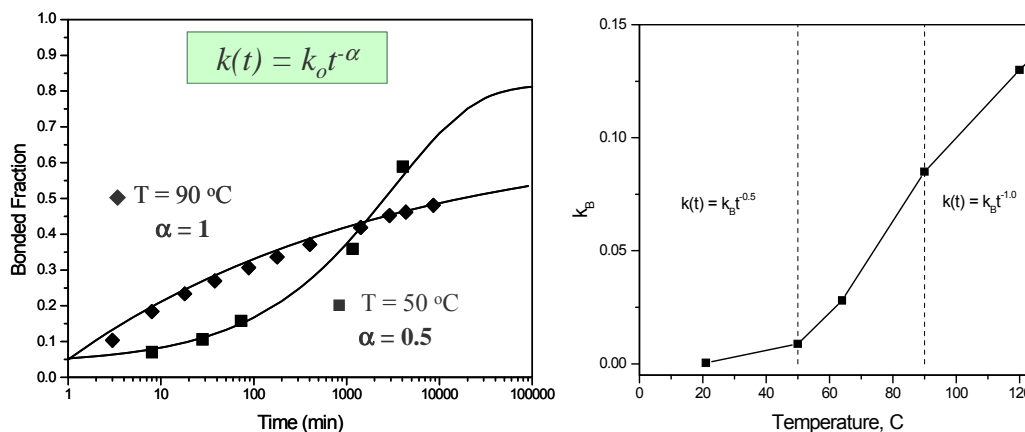


Fig. 3-12: (Left) Representative kinetic data for the bonding of PFPE-OH (tradename: Fomblin Zdol[®]) to amorphous carbon at $T = 50^\circ\text{C}$ and $T = 90^\circ\text{C}$. Solid lines represent fits using a rate coefficient of the form $k(t) = k_b t^{-\alpha}$ with $\alpha = 0.5$ for $T = 50^\circ\text{C}$ and $\alpha = 1.0$ for $T = 90^\circ\text{C}$. (Right) Change in bonding rate constants k_B . Temperature dependence of the initial bonding rate constants for a 10.5 Å PFPE-OH film. Vertical lines delineate the non-classical kinetic regimes.

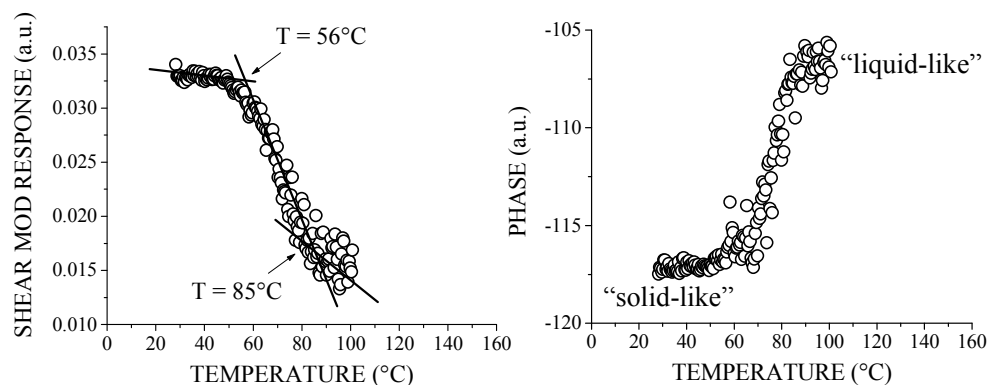


Fig. 3-13: SM-FM Analysis on Zdol: (Left) Amplitude response reveals three regimes as found in the kinetic studies. (Right) Parallel measured out of phase response identifies the material phase as frozen below 50°C and in a liquid-like melt state above 90°C .

Currently, very limited research is conducted in analyzing reaction processes at interfaces with intrinsic thermomechanical material properties. Typical approaches are limited to statistical considerations and oversimplified rate models. This research illustrates the importance of the underlying molecular mobility on the reaction kinetics. As the molecular mobility within a condensed phase can be affected by a variety of physical constraints (internal, external, size, etc.), it is imperative to expand our efforts in investigation local thermomechanical properties, as it was illustrated in this section, and throughout the entire document.

6. References and Citations Therein

- ¹ D. B. Knorr, T. Gray, and R. M. Overney, *Cooperative and Submolecular Dissipation Mechanisms of Sliding Friction in Complex Organic Systems*, J. Chem. Phys. **129**, 074504 (2008).
- ² M. Y. He, A. S. Blum, G. Overney, and R. M. Overney, *Effect of interfacial liquid structuring on the coherence length in nanolubrication*, Physical Review Letters **88**, 154302 (2002).
- ³ T. Gray, T. D. Kim, D. B. Knorr, J. D. Luo, A. K. Y. Jen, and R. M. Overney, *Mesoscale dynamics and cooperativity of networking dendronized nonlinear optical molecular glasses*, Nano Letters **8**, 754-9 (2008).
- ⁴ D. B. Knorr, T. Gray, and R. M. Overney, *Intrinsic Friction Analysis - Novel Nanoscopic Access to Molecular Mobility in Constrained Organic Systems*, Ultramicroscopy **in press** (2008).
- ⁵ R. M. Overney, E. Meyer, J. Frommer, D. Brodbeck, R. Luthi, L. Howald, H. J. Guntherodt, M. Fujihira, H. Takano, and Y. Gotoh, *Friction Measurements on Phase-Separated Thin-Films with a Modified Atomic Force Microscope*, Nature **359**, 133-5 (1992).
- ⁶ T. Gray, R. M. Overney, M. Haller, J. Luo, and A. K. Y. Jen, *Low temperature relaxations and effects on poling efficiencies of dendronized nonlinear optical side-chain polymers*, Applied Physics Letters **86** (2005).
- ⁷ S. Sills, R. M. Overney, W. Chau, V. Y. Lee, R. D. Miller, and J. Frommer, *Interfacial glass transition profiles in ultrathin, spin cast polymer films*, Journal of Chemical Physics **120**, 5334-8 (2004).
- ⁸ S. Sills, T. Gray, and R. M. Overney, *Molecular dissipation phenomena of nanoscopic friction in the heterogeneous relaxation regime of a glass former*, Journal of Chemical Physics **123** (2005).
- ⁹ R. Overney and E. Meyer, *Tribological Investigations Using Friction Force Microscopy*, Mat. Res. Soc. Bulletin **18**, 26-34 (1993).
- ¹⁰ T. Gray, J. Killgore, J. D. Luo, A. K. Y. Jen, and R. M. Overney, *Molecular mobility and transitions in complex organic systems studied by shear force microscopy*, Nanotechnology **18** (2007).
- ¹¹ R.M. Overney and S. E. Sills, in *Interfacial Properties on the Submicron Scale*, edited by J. Frommer and R. M. Overney (Oxford Univ. Press, New York, 2001), p. 2-23.
- ¹² R. M. Overney, D. P. Leta, L. J. Fetters, Y. Liu, M. H. Rafailovich, and J. Sokolov, *Dewetting dynamics and nucleation of polymers observed by elastic and friction force microscopy*, Journal of Vacuum Science & Technology B **14**, 1276-9 (1996).
- ¹³ R. M. Overney, G. Tindall, and J. Frommer, in *Handbook of Nanotechnology*, edited by B. Bhushan (1439-1453, Heidelberg, 2007).
- ¹⁴ S. R. Ge, L. T. Guo, M. H. Rafailovich, J. Sokolov, R. M. Overney, C. Buenviaje, D. G. Peiffer, and S. A. Schwarz, *Wetting behavior of graft copolymer substrate with chemically identical homopolymer films*, Langmuir **17**, 1687-92 (2001).
- ¹⁵ A. Karim, T. M. Slawacki, S. K. Kumar, J. F. Douglas, S. K. Satija, C. C. Han, T. P. Russell, Y. Liu, R. Overney, O. Sokolov, and M. H. Rafailovich, *Phase-separation-induced surface patterns in thin polymer blend films*, Macromolecules **31**, 857-62 (1998).
- ¹⁶ C. Buenviaje, S. R. Ge, M. Rafailovich, J. Sokolov, J. M. Drake, and R. M. Overney, *Confined flow in polymer films at interfaces*, Langmuir **15**, 6446-50 (1999).
- ¹⁷ R. M. Overney, C. Buenviaje, R. Luginbuhl, and F. Dinelli, *Glass and structural transitions measured at polymer surfaces on the nanoscale*, Journal of Thermal Analysis and Calorimetry **59**, 205-25 (2000).
- ¹⁸ S. Ge, Y. Pu, W. Zhang, M. Rafailovich, J. Sokolov, C. Buenviaje, R. Buckmaster, and R. M. Overney, *Shear modulation force microscopy study of near surface glass transition temperatures*, Physical Review Letters **85**, 2340-3 (2000).
- ¹⁹ E. Meyer, R. Overney, R. Luthi, D. Brodbeck, L. Howald, J. Frommer, H. J. Guntherodt, O. Wolter, M. Fujihira, H. Takano, and Y. Gotoh, *Friction Force Microscopy of Mixed Langmuir-Blodgett-Films*, Thin Solid Films **220**, 132-7 (1992).
- ²⁰ E. Meyer, R. Overney, D. Brodbeck, L. Howald, R. Luthi, J. Frommer, and H. J. Guntherodt, *Friction and Wear of Langmuir-Blodgett-Films Observed by Friction Force Microscopy*, Physical Review Letters **69**, 1777-80 (1992).
- ²¹ L. Howald, R. Luthi, E. Meyer, G. Gerth, H. G. Haefke, R. Overney, and H. J. Guntherodt, *Friction Force Microscopy on Clean Surfaces of NaCl, NaF, and AgBr*, Journal of Vacuum Science & Technology B **12**, 2227-30 (1994).
- ²² R. M. Overney, T. Bonner, E. Meyer, M. Reutschi, R. Luthi, L. Howald, J. Frommer, H. J. Guntherodt, M. Fujihira, and H. Takano, *Elasticity, Wear, and Friction Properties of Thin Organic Films Observed with Atomic-Force Microscopy*, Journal of Vacuum Science & Technology B **12**, 1973-6 (1994).

- ²³ R. M. Overney, H. Takano, M. Fujihira, W. Paulus, and H. Ringsdorf, *Anisotropy in Friction and Molecular Stick-Slip Motion*, Physical Review Letters **72**, 3546-9 (1994).
- ²⁴ R. M. Overney, H. Takano, and M. Fujihira, *Elastic Compliances Measured by Atomic-Force Microscopy*, Europhysics Letters **26**, 443-7 (1994).
- ²⁵ R. M. Overney, H. Takano, M. Fujihira, E. Meyer, and H. J. Guntherodt, *Wear, Friction and Sliding Speed Correlations on Langmuir-Blodgett-Films Observed by Atomic-Force Microscopy*, Thin Solid Films **240**, 105-9 (1994).
- ²⁶ F. Dinelli, C. Buenviaje, and R. M. Overney, *Glass transitions of thin polymeric films: Speed and load dependence in lateral force microscopy*, Journal of Chemical Physics **113**, 2043-8 (2000).
- ²⁷ C. Buenviaje, F. Dinelli, and R. M. Overney, *Investigations of heterogeneous ultrathin blends using lateral force microscopy*, Macromolecular Symposia **167**, 201-12 (2001).
- ²⁸ S. Sills and R. M. Overney, *Creeping friction dynamics and molecular dissipation mechanisms in glassy polymers*, Physical Review Letters **91**, 095501 (2003).
- ²⁹ S. Sills, H. Fong, C. Buenviaje, M. Sarikaya, and R. M. Overney, *Thermal transition measurements of polymer thin films by modulated nanoindentation*, Journal of Applied Physics **98** (2005).
- ³⁰ S. Sills, T. Gray, J. Frommer, and R. M. Overney, in *Applications of Scanned Probe Microscopy to Polymers*, (2005), Vol. 897, p. 98-111.
- ³¹ S. Sills, R. M. Overney, B. Gotsmann, and J. Frommer, *Strain shielding and confined plasticity in thin polymer films: Impacts on thermomechanical data storage*, Tribology Letters **19**, 9-15 (2005).
- ³² J. P. Killgore and R. M. Overney, *Interfacial mobility and bonding strength in nanocomposite thin film membranes*, Langmuir **24**, 3446-51 (2008).
- ³³ R. M. Overney, D. P. Leta, C. F. Pictroski, M. H. Rafailovich, Y. Liu, J. Quinn, J. Sokolov, A. Eisenberg, and G. Overney, *Compliance measurements of confined polystyrene solutions by atomic force microscopy*, Physical Review Letters **76**, 1272-5 (1996).
- ³⁴ M. Y. He, A. S. Blum, D. E. Aston, C. Buenviaje, R. M. Overney, and R. Luginbuhl, *Critical phenomena of water bridges in nanoasperity contacts*, Journal of Chemical Physics **114**, 1355-60 (2001).
- ³⁵ S. Sills, K. Vorvolakos, M.K. Chaudhury, and R. M. Overney, in *Friction and Wear on the Atomic Scale*, edited by E. Gnecco and E. Meyer (Springer Verlag, Heidelberg, 2007), p. 659-76.
- ³⁶ E. Meyer, L. Howald, R. M. Overney, H. Heinzelmann, J. Frommer, H. J. Guntherodt, T. Wagner, H. Schier, and S. Roth, *Molecular-Resolution Images of Langmuir-Blodgett-Films Using Atomic Force Microscopy*, Nature **349**, 398-400 (1991).
- ³⁷ R. Luthi, R. M. Overney, E. Meyer, L. Howald, D. Brodbeck, and H. J. Guntherodt, *Measurements on Langmuir-Blodgett-Films by Friction Force Microscopy*, Helvetica Physica Acta **65**, 866-7 (1992).
- ³⁸ F. Schabert, A. Hefti, K. Goldie, A. Stemmer, A. Engel, E. Meyer, R. Overney, and H. J. Guntherodt, *Ambient-Pressure Scanning Probe Microscopy of 2d Regular Protein Arrays*, Ultramicroscopy **42**, 1118-24 (1992).
- ³⁹ J. Frommer, R. Luthi, E. Meyer, D. Anselmetti, M. Dreier, R. Overney, H. J. Guntherodt, and M. Fujihira, *Adsorption at Domain Edges*, Nature **364**, 198- (1993).
- ⁴⁰ R. M. Overney, E. Meyer, J. Frommer, H. J. Guntherodt, M. Fujihira, H. Takano, and Y. Gotoh, *Force Microscopy Study of Friction and Elastic Compliance of Phase-Separated Organic Thin-Films*, Langmuir **10**, 1281-6 (1994).
- ⁴¹ R. M. Overney, manuscript in preparation.
- ⁴² T. Gray, C. Buenviaje, R. M. Overney, S. A. Jenekhe, L. X. Zheng, and A. K. Y. Jen, *Nanorheological approach for characterization of electroluminescent polymer thin films*, Applied Physics Letters **83**, 2563-5 (2003).
- ⁴³ T. D. Kim, J. W. Kang, J. D. Luo, S. H. Jang, J. W. Ka, N. Tucker, J. B. Benedict, L. R. Dalton, T. Gray, R. M. Overney, D. H. Park, W. N. Herman, and A. K. Y. Jen, *Ultralarge and thermally stable electro-optic activities from supramolecular self-assembled molecular glasses*, Journal of the American Chemical Society **129**, 488-9 (2007).
- ⁴⁴ J. H. Wei, M. Y. He, and R. M. Overney, *Direct measurement of nanofluxes and structural relaxations of perfluorinated ionomer membranes by scanning probe microscopy*, Journal of Membrane Science **279**, 608-14 (2006).
- ⁴⁵ J. P. Killgore, W. King, K. Kjoller, and R. M. Overney, *Heated-tip AFM: Applications in Nanocomposite Polymer Membranes and Energetic Materials*, Microscopy Today **15**, 20-5 (2007).